Biosensors and Bioelectronics 142 (2019) 111486

Contents lists available at ScienceDirect

Biosensors and Bioelectronics

journal homepage: www.elsevier.com/locate/bios

A novel enzyme-free electrochemical biosensor for rapid detection of *Pseudomonas aeruginosa* based on high catalytic Cu-ZrMOF and conductive Super P

Xin Zhang[a], Guoming Xie[b], Dan Gou[a], Peng Luo[a], Yuan Yao[a], Hui Chen[a,*]

[a] Clinical Laboratories, The First Affiliated Hospital of Chongqing Medical University, Chongqing, 400016, PR China
[b] Key Laboratory of Laboratory Medical Diagnostics, Chinese Ministry of Education, Department of Laboratory Medicine, Chongqing Medical University, Chongqing, 400016, PR China

ARTICLE INFO

Keywords:
Electrochemical biosensor
Metal-organic framework
Super P
P. aeruginosa
Gold nanoparticles

ABSTRACT

Pseudomonas aeruginosa (*P. aeruginosa*) is one of the most intractable multidrug-resistant bacteria of nosocomial infections. The conventional detection methods for *P. aeruginosa* are time-consuming or low detection sensitivity. Here, a novel enzyme-free electrochemical biosensor was constructed to detect *P. aeruginosa* rapidly and sensitively. Firstly, the ZrMOF with large surface area was synthesized, which offers excellent adsorption. Further, it was connected with a specific amount of Cu^{2+} to synthesize Cu-ZrMOF with high catalytic activity. Then the Cu-ZrMOF@Aptamer@DNA nanocomposite was composed and served as the signal probe to catalyse the decomposition of H_2O_2. Moreover, high conductive Super P was introduced to increase the electron transfer for satisfactory detection sensitivity. The proposed biosensor was constructed and used to quantify *P. aeruginosa* with a wide linearity range of 10–10^6 CFU mL^{-1} and a low limit of detection of 2 CFU mL^{-1} (S/N = 3). Compared with conventional methods, the new method of present biosensor is more sensitive, and less time-consuming (only within 120 min). The analytical performance evaluation indicated that the biosensor exhibits good reproducibility and specificity. Finally, the biosensor was successfully applied to quantify *P. aeruginosa* in spiked urine samples. These results show that the proposed electrochemical biosensor might be a potential laboratory tool for detecting *P. aeruginosa* in the clinic.

1. Introduction

P. aeruginosa is one of the top three pathogens involved in opportunistic infections (Tang et al., 2017). *P. aeruginosa* was listed as a critical pathogen by the World Health Organization in 2017. It can cause a variety of infections in immunocompromised patients, such as urinary tract, blood and respiratory infections (Jia et al., 2017; Shah and Naseby, 2015). Prompt diagnosis and correct treatment depend on the results of laboratory detection. At present, conventional detection methods for *P. aeruginosa* include plate culture, polymerase chain reaction (PCR) and mass spectrometry. As the gold standard, the plate culture is accurate but time-consuming (Ito et al., 2018). Although quantitative detection of *P. aeruginosa* can be achieved by PCR, the requirement for operators is quite high (Kunze et al., 2016). In addition, mass spectrometry requires expensive and large-scale instruments (Mougous et al., 2006). Therefore, it is important and urgent to discover a rapid, simple and sensitive method to detect *P. aeruginosa*.

Recently, biosensor has attracted increasing attention in the detection of *P. aeruginosa*. For example, a localized surface plasmon resonance aptasensor was put forward to detect *P. aeruginosa* (Hu et al., 2018). Yue et al. reported a label-free electrochemiluminescent biosensor for detection of *P. aeruginosa* using phage with strict host specificity as specific recognition element, yet the operation process was relatively complicated (Yue et al., 2017). An electrochemical immunoassay for detection of *P. aeruginosa* based on pectin-gold nanocomposite had also been reported, but the sensitivity was not satisfactory (Krithiga et al., 2016). These mentioned methods of biosensor can overcome some defects of the conventional methods to a certain degree. However, the low signal amplification efficiency, as a key issue, still cannot meet the clinical needs, this limits their clinical application. Therefore, it is necessary to provide a more sensitive and effective biosensor to detect *P. aeruginosa* in the clinic.

It is well known that the electrochemical biosensor has been an attractive tool. It offers many outstanding advantages including rapid

* Corresponding author. The First Affiliated Hospital of Chongqing Medical University, No. 1, You Yi Road, Yu-zhong District, Chongqing, 400016, PR China.
E-mail address: huichen@cqmu.edu.cn (H. Chen).

https://doi.org/10.1016/j.bios.2019.111486
Received 23 April 2019; Received in revised form 26 June 2019; Accepted 28 June 2019
Available online 29 June 2019
0956-5663/

analysis, high sensitivity, low cost, easy operation and miniaturization (Li et al., 2018). With the development of nanoscience and nanotechnology, nanomaterials have been increasingly used to construct the electrochemical biosensor (Li et al., 2017; Tang et al., 2018). Carbon-based nanomaterials such as graphene oxide, nitrogen-doped graphene and carbon black play an important role in nanotechnology owing to their excellent chemical and physical features, such as strong adsorption capability, low cost and easy preparation (da Silva et al., 2018). Among them, Super P, a type of carbon black with high chemical stability, can produce more stable detection signal. More important, it has high conductivity and can be used to increase current signal by modifying electrode. However, research based on Super P for detection is rarely reported. It is well known that gold nanoparticles (AuNPs) present good biocompatibility and conductivity. Furthermore, they can provide enough binding sites for subsequent proteins (Huo et al., 2016). Therefore, in present work, both Super P and AuNPs were connected onto the surfaces of the electrodes to increase the current signal for satisfactory detection sensitivity.

Metal-organic framework (MOF) materials are another vital element of signal amplification. As a new type of crystal mesoporous materials, MOFs have attracted considerable attention in biosensor due to its merits of controllable structure, large surface area and adjustable aperture (Kaneti et al., 2017). Among them, zirconium series metal-organic framework (ZrMOF) displays great potential. Recently, Yan et al. constructed a chemiluminescent biosensor to analyse protein kinase activity by loading specific amounts of Au and Pt nanoparticles on the large surface area of ZrMOF (Yan et al., 2018). Of note, due to the presence of the Zr–O group in ZrMOF, the aptamer modified by phosphate groups (P) can be bound to ZrMOF through Zr–O–P (Wang et al., 2017a,b), which is conducive to biosensor construction. Guo et al. reported an electrochemical biosensor for detecting carcinoembryonic antigens based on Zr–O–P (Guo et al., 2017). Furthermore, owing to the outstanding adsorptive ability and various grafting groups, including $–NH_2$ and –COOH (He et al., 2014), the ZrMOF is considered as an ideal candidate for that it can immobilize both metal ions and biological ligands. Based on the different metal ions (Pb^{2+} or Cd^{2+}) carried by ZrMOF, Chen et al. proposed a new biosensor to detect multiple antibiotics (Chen et al., 2017). Therefore, the ZrMOF possesses many advantages and can be a perfect candidate in the construction of biosensor. In present work, the Cu-ZrMOF with high catalytic activity was successfully synthesized, and it was applied to construct bacterial biosensor.

Aptamers, known as “artificial antibodies”, are short, single-stranded oligonucleotides or peptide sequences. They have the virtues of high affinity and specificity towards targets, easy preparation, low cost and excellent stability (Meng et al., 2016). In previous work, the aptamer was used as recognition element for the detection of staphylococcal enterotoxin B (Zhou et al., 2016) and *Mycobacterium tuberculosis* secreted protein MPT64 (Gou et al., 2018), respectively. Herein, a new enzyme-free electrochemical biosensor has been designed to detect *P. aeruginosa* rapidly and sensitively. Firstly, the Cu-ZrMOF with high catalytic activity was synthesized by connecting the ZrMOF and a specific amount of Cu^{2+}. Then the Cu-ZrMOF@Aptamer@DNA nanocomposite was composed and served as the signal probe by catalysing the decomposition of H_2O_2. The aptamer was used to identify *P. aeruginosa* specifically, and the short DNA was connected to the remaining binding sites of Cu-ZrMOF, which can facilitate the recognition of *P. aeruginosa* by exposing the base sequences of the aptamer. Moreover, the high conductive Super P was introduced to increase the electron transfer for satisfactory detection sensitivity. To the best of our knowledge, the innovative combination of Cu-ZrMOF and Super P is rarely reported in the field of electrochemical biosensor. As a kind of materials with excellent conductivity, AuNPs were used to immobilize antibody on electrode surface in present work. The stepwise fabrication process and assay principle were depicted in Scheme 1. As expected, an enhanced current signal could be detected only in the existance of *P. aeruginosa*.

2. Materials and methods

2.1. Reagents and materials

P. aeruginosa (ATCC 27853) was obtained from the American Type Culture Collection (ATCC, USA). *Escherichia coli* (*E. coli*), *Staphylococcus aureus* (*S. aureus*), *Acinetobacter baumannii* (*A. baumannii*), and *Klebsiella pneumoniae* (*K. pneumoniae*) were gifted from the First Affiliated Hospital of Chongqing Medical University. Mouse monoclonal antibody [B11] (ab35835) against *P. aeruginosa* was ordered from Abcam Co. (Cambridge, UK). Super P was obtained from TIMCAL (Henan, China). Copper (II) chloride dihydrate ($CuCl_2.2H_2O$) was purchased from Sigma-Aldrich (St. Louis, MO, USA). Zirconium (IV) chloride ($ZrCl_4$), 2, 2′-bipyridine-5, 5′-dicarboxylic acid (bpydc) and acetic acid (HAc, 99.95%) were obtained from Aladdin (Shanghai, China). Chloroauric acid ($HAuCl_4$) and anhydrous tetrahydrofuran (THF) were obtained from Macklin (Shanghai, China). Dimethylformamide (DMF) was purchased from Chron Chemicals (Sichuan, China). Chitosan, sodium citrate, tryptone, yeast extract, and bovine serum albumin (BSA, 96%–99%) were purchased from Sangon Biotechnology, Co. (Shanghai, China). All the oligonucleotide sequences were synthesized and purified by high-performance liquid chromatography at Sangon Biotechnology, Co. (Shanghai, China). The sequences are listed in Table S1. Ultrapure water (MilliQ 18.2 MΩ cm, Millipore System, Inc) was employed in all of the experiments. All other reagents used in this work were of analytical grade and were utilized without further purification.

2.2. Apparatus

Cyclic voltammetry (CV), electrochemical impedance spectroscopy (EIS) and differential pulse voltammetry (DPV) were carried out on a CHI 660E electrochemical workstation (Shanghai, China) with a conventional three-electrode system consisting of a modified gold electrode as the working electrode, an Ag/AgCl electrode (immersed in saturated KCl solution) as the reference electrode, and a Pt wire as the auxiliary electrode. Cary eclipse fluorescence spectrophotometer (Agilent, California) and upright fluorescence microscopy (Nikon ECLIPSE 80i, Japan) were used to analyse the recognition effect between the aptamer and *P. aeruginosa*. High-resolution scanning electron microscopy (HR-SEM, FEI Nova Nano 450, USA) and high-resolution transmission electron microscopy (HR-TEM, FEI G2F20, USA) were conducted to characterize the morphology of ZrMOF. Transmission electron microscopy (TEM, FEI G2F20, USA) and field emission scanning electron microscopy (FESEM, Quanta 400 FEG, USA) were employed to characterize AuNPs and Super P, respectively. Energy dispersive spectrometer (EDS, Oxford X-MaxN, Britain) was used to analyse the elements of the Cu-ZrMOF. Zeta potential (Nano ZS (zen3600), UK) was used to analyse whether aptamer and DNA were attached onto the surface of Cu-ZrMOF.

2.3. Preparation of super P and AuNPs

Firstly, to obtain the highly uniform Super P suspension (1 mg mL^{-1}), 4.0 mg Super P was dispersed into 4.0 mL chitosan solution (0.5%) via sonication for 1 h. AuNPs were prepared according to procedures described in the literature (Yang et al., 2016). Briefly, 100 mL $HAuCl_4$ (0.01%) was stirred and boiled for 15 min, then 1 mL trisodium citrate (2%) was slowly added to the above solution. The mixture solution was stirred continuously for another 5 min until the colour was changed from pale yellow to wine red. Finally, the AuNPs solution was cooled to room temperature (RT) and stored at 4 °C for subsequent usage.

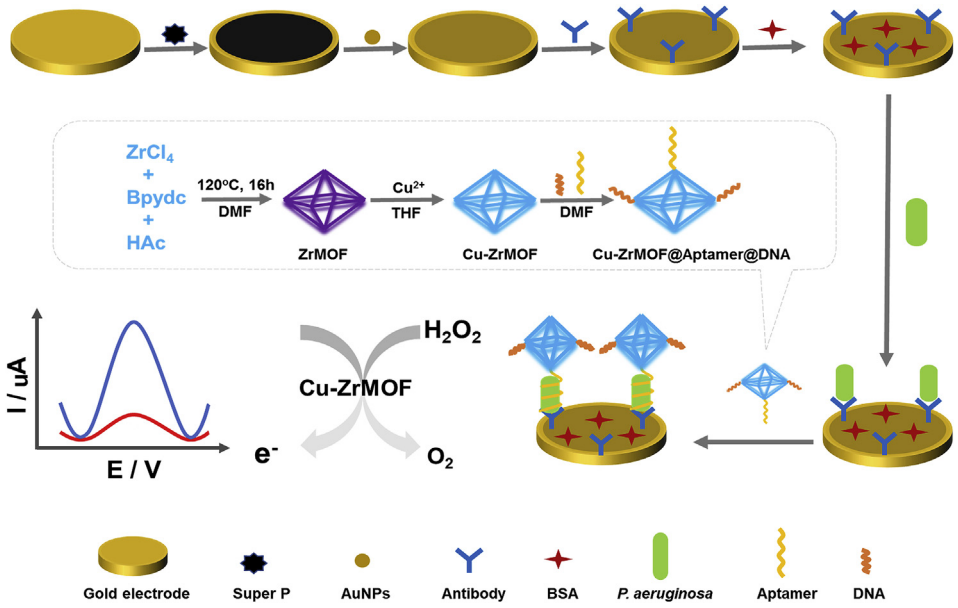

Scheme 1. Schematic of the electrochemical detection of *P. aeruginosa*.

2.4. Synthesis of ZrMOF, Cu-ZrMOF, and Cu-ZrMOF@Aptamer@DNA

2.4.1. Preparation of ZrMOF

ZrMOF was prepared according to procedures described in the literature (Chen et al., 2018) with minor modification. Firstly, 80 mg bpydc was dispersed in 6 mL DMF with sonication for 5 min, and then 26.12 mg $ZrCl_4$ was dissolved in 12 mL DMF with sonication for 5 min. Afterwards, the two reactants were mixed together in the reactor, then 1.5 mL acetic acid was added with sonication for 5 min. The mixture solution was then stirred and heated at 120 °C for 16 h. Finally, the white solid was obtained by centrifuging at 9,000 rpm (5,450 rcf) for 10 min and washed three times with ethyl alcohol.

2.4.2. Synthesis of Cu-ZrMOF

Cu-ZrMOF was synthesized according to procedures described in the literature (Chen et al., 2018) with minor modification. In a round-bottom flask, 30 mg ZrMOF was dissolved in 5 mL THF with sonication for 5 min, 10.60 mg $CuCl_2.2H_2O$ was added to the ZrMOF solution with sonication for 5 min, and then the mixture was stirred for 2 h at RT. Finally, the green solid was collected by centrifugation at 9,000 rpm (5,450 rcf) for 5 min and washed three times with ethyl alcohol, then re-suspended with 2 mL DMF to obtain the Cu-ZrMOF solution. The solution was stored at 4 °C in the dark for subsequent usage.

2.4.3. Preparation of Cu-ZrMOF@Aptamer@DNA

Immobilization of aptamer and DNA onto Cu-ZrMOF was completed according to the literature (Liu et al., 2018) with little modification. Firstly, 100 μL the abovementioned Cu-ZrMOF solution was centrifuged at 9,000 rpm (5,450 rcf) for 5 min, the supernatant was discarded, and the leftover was resuspended with 460 μL DMF. Then, 20 μL aptamer (10 μmol L^{-1}) and 20 μL DNA (10 μmol L^{-1}) in PBS (0.01 mol L^{-1}, pH 7.4) were added into Cu-ZrMOF solution, the mixture was stirred well at 37 °C overnight. Cu-ZrMOF@Aptamer@DNA was then purified by three circles of centrifugation at 9,000 rpm (5,450 rcf) for 5 min and washed with ethyl alcohol. Finally, the product was stored in 100 μL DMF as signal probe for future use.

2.5. Fabrication of the electrochemical biosensor

To obtain a mirror-like surface of the gold electrode, the preparation procedures were performed as follows: Firstly, gold electrode was polished with 0.3 μm and 0.05 μm alumina slurry followed by ultrasonic cleaning in ultrapure water, ethyl alcohol and ultrapure water, successively, for 5 min. Next, the gold electrode was treated with freshly prepared piranha solution (98% H_2SO_4:30% H_2O_2, 3:1 v/v), followed by rinsing thoroughly with ultrapure water. At last, a mirror-like surface of the gold electrode was obtained. Then, 10 μL Super P (1 mg mL^{-1}) was dropped onto the prepared bare gold electrode and dried at RT, and 9 μL AuNPs was added and dried at 37 °C for 1 h. Following, 8 μL antibody against *P. aeruginosa* (50 μg mL^{-1}) in PBS (0.01 mol L^{-1}, pH 7.4) was attached directly onto the gold electrode surface at 37 °C for 2 h. After washing with PBS (0.01 mol L^{-1}, pH 7.4), 10 μL BSA (0.5%) was applied to block the unbound binding sites on the surface of the gold electrode at RT for 1 h. Finally, the proposed electrochemical biosensor was obtained after another round of washing with PBS, and it was stored in PBS (0.01 mol L^{-1}, pH 7.4) at 4 °C for future use.

2.6. Experiment on the specific binding ability of the aptamer and P. aeruginosa

To investigate the specific binding ability of the aptamer and *P. aeruginosa*, *S. aureus* was chosen as control. Both *P. aeruginosa* and *S. aureus* were incubated with FAM-labelled aptamer (200 nmol L^{-1}) in PBS (0.01 mol L^{-1}, pH 7.4) at 37 °C for 4 h, respectively. After centrifuging at 5,000 rpm (1,680 rcf) for 5 min, the fluorescence intensity of the two different reaction system sediments was observed by fluorescence microscopy. The fluorescence intensity of the supernatant was measured by fluorescence spectrophotometer (excitation and emission wavelengths: 490 nm and 520 nm, respectively; excitation and emission slits: 5 nm and 5 nm, respectively).

2.7. Preparation of bacterial strains

Five hundred milliliters Luria-Bertani (LB) medium solution was prepared consisting of 5 g sodium chloride, 5 g tryptone, 2.5 g yeast extract, 7.5 g agarose G-10 and 500 mL ddH_2O. All bacterial strains were incubated freshly with LB plates in an incubator containing 5% CO_2 at 37 °C for 16–24 h. McFarland turbidimetry was applied to quantify *P. aeruginosa*. The bacterial suspensions with different concentrations (10, 10^2, 10^3, 10^4, 10^5 and 10^6 CFU mL^{-1}) were prepared with PBS (0.01 mol L^{-1}, pH 7.4).

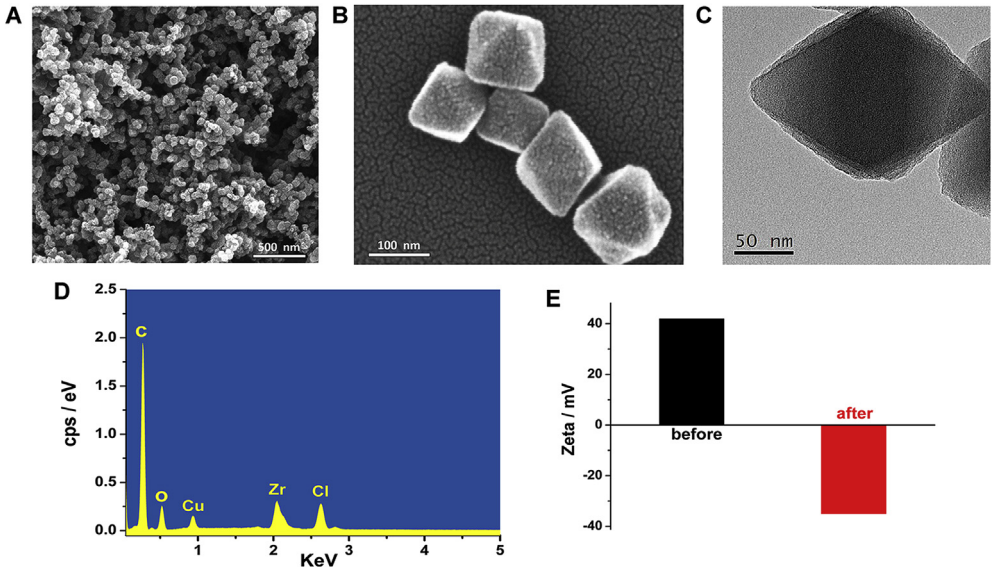

Fig. 1. Characterization of the materials: (A) FE-SEM image of Super P. (B) HR-SEM image of ZrMOF. (C) HR-TEM image of ZrMOF. (D) EDS pattern of Cu-ZrMOF. (E) Zeta potential of Cu-ZrMOF before and after modifying by aptamer and DNA.

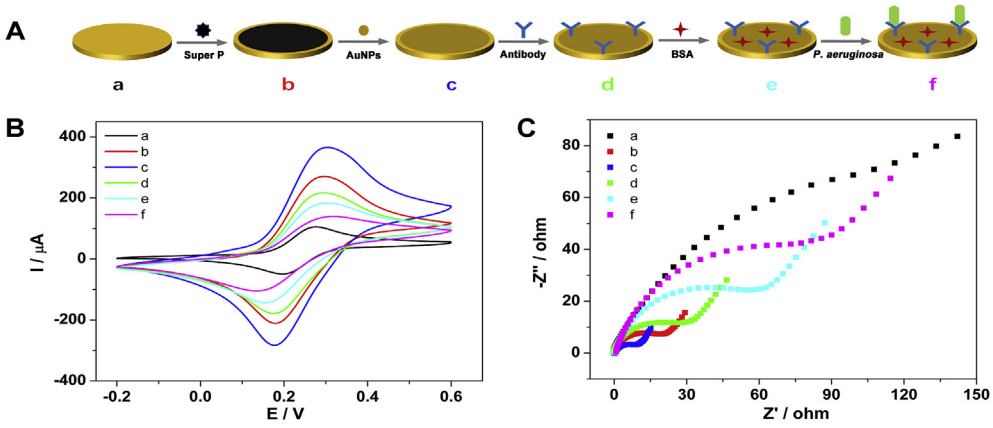

Fig. 2. CV and EIS curves during the fabricative process of the electrochemical biosensor: (A) Fabricative process of the working electrode. (B) Curve of CV step by step. (C) Curve of EIS step by step: (a) bare gold electrode, (b) Super P/gold electrode, (c) AuNPs/Super P/gold electrode, (d) antibody/AuNPs/Super P/gold electrode, (e) BSA/antibody/AuNPs/Super P/gold electrode, (f) *P. aeruginosa*/BSA/antibody/AuNPs/Super P/gold electrode. (For interpretation of the references to colour in this figure legend, the reader is referred to the Web version of this article.)

2.8. Electrochemical detection of P. aeruginosa

Ten microliters solution of *P. aeruginosa* with different concentrations was added onto the prepared electrode and incubated at RT for 1 h. After washing with PBS, 10 μL signal probe (Cu-ZrMOF@Aptamer@DNA) was added for further immunoreaction and signal detection. DPV measurements were performed from −0.1 V to +0.6 V in PBS (0.01 mol L^{-1}, pH 5.0) containing H_2O_2 (0.02 mmol L^{-1}, 30%).

3. Results and discussion

3.1. Characterization of the materials

FE-SEM and TEM were employed to evaluate the surface morphology of Super P and AuNPs, respectively. As seen in Fig. 1A, the microparticles of Super P were distributed uniformly with about size of 70 nm. The nanocrystals were sphere and had a large surface area, which indicated that Super P had the potential to increase the electrode effective surface and improve electrical conductivity. Fig. S1 showed that the synthetic AuNPs were dispersed homogeneously with an average diameter size of 15 nm. The structure and morphology of ZrMOF were investigated using HR-SEM and HR-TEM. As depicted in Fig. 1B and C, the crystal morphology of ZrMOF was a typical octahedral structure with an average size of 120 nm, which implied that ZrMOF had good dispersibility. These results indicated that the AuNPs and ZrMOF were prepared successfully. The presence and content of the elements of Cu-ZrMOF were analysed by EDS. As shown in Fig. 1D, the peaks of Zr, Cu, Cl, C and O were clearly observed, and the peak intensity of Cu was obvious, which indicated that Cu^{2+} was connected to ZrMOF successfully. The zeta potential is used to characterize the process of modification and the stability of prepared composites (Liu et al., 2018). The potential value of Cu-ZrMOF solution was +42 mV, the potential value was decreased to −35 mV measured in the same solution upon connecting of the negatively charged aptamer and DNA (Fig. 1E). It indicated that aptamer and DNA were connected onto the surface of Cu-ZrMOF successfully. According to El-Naggar's report, the particles in solution with zeta potential above +25 mV and below −25 mV are considered to be stable (El-Naggar et al., 2016). In fact, the zeta potential of prepared composites was just in this range. This implied that the Cu-ZrMOF@Aptamer@DNA had good stability and might be an ideal signal probe.

3.2. Characterization of stepwise fabrication of the electrochemical biosensor

The preparation of the electrochemical biosensor was shown step by step in Fig. 2A. As a convenient and effective method, CV measurement was used to investigate the process of fabrication by measuring the current signal with a scan rate of 0.1 V/S in PBS (0.01 mol L^{-1}, pH 7.4)

containing 5 mmol L^{-1} $[Fe(CN)6]^{3-/4-}$ and 0.10 mol L^{-1} KCl. As shown in Fig. 2B, the bare gold electrode (curve a) exhibited a well-defined redox peak. When Super P (curve b) was fixed onto the bare gold electrode, the current signal was increased obviously. It indicated that Super P had good conductivity. Next, AuNPs (curve c) were modified on the gold electrode, and the current signal continued to increase, it might be caused by the enhancement of effective surface area of gold electrode with the help of AuNPs. Modified by nonconductive substances, such as the antibody, BSA and *P. aeruginosa*, the current signals of the modified electrodes decreased gradually for that the electron transfer was hindered. It is supported by Li's report (Li et al., 2018). When the antibody was added onto the electrode, the current signal decreased, it indicated that the antibody (curve d) was immobilized onto the electrode surface successfully. According to the literature, it might be connected by the Au–NH_2 bond (Wang et al., 2017a,b). The current signal was decreased further after BSA (curve e) was fixed on the electrode. Lastly, the redox peak was decreased drastically (curve f), which implied the specific recognition of antibody and *P. aeruginosa*.

As another common method for studying the interfacial properties at the electrode surface, EIS (low frequency: 1 Hz) was applied to evaluate the feasibility of the electrochemical biosensor. As depicted in Fig. 2C, a tiny circuit electron transfer resistance (Ret) indicated that the bare gold electrode had admirable electron-transfer capability (curve a). After assembling with Super P, the Ret was decreased (curve b). With further modification by AuNPs, the Ret even was further decreased (curve c). However, the Ret was increased gradually after connecting the antibody (curve d), BSA (curve e) and *P. aeruginosa* (curve f) on the surface of gold electrode step by step. This showed that the antibody, BSA and *P. aeruginosa* were successfully immobilized onto the gold electrode surface. The relative small Ret change is probably due to the modified Super P and AuNPs with high conductivity. This evidence suggested that the proposed biosensor was feasible.

3.3. Feasibility of the proposed electrochemical biosensor

To evaluate the effect of Super P on conductivity, the current signal value was tested by CV measurement. In Fig. 3A, the current signal was significantly increased after modification of Super P, which was about three times that of the bare gold electrode. The effect of increasing conductivity was obviously higher than that of recent reports (Hassani et al., 2018; Zhang et al., 2019). This indicated that Super P could increase the current signal and assist to get satisfactory detection sensitivity. As seen in Fig. 3B, distinct and consistent DPV current signals were observed when Cu-ZrMOF and Cu-ZrMOF@Aptamer@DNA were cast onto the surface of gold electrode. It suggested that both of them had excellent catalytic activity. The catalytic activity of Cu-ZrMOF was not reduced after being modified by aptamer and DNA. As shown in Fig. 3C, no distinct DPV current signals were observed when Super P (curve a), AuNPs (curve b), antibody (curve c), BSA (curve d) and *P. aeruginosa* (curve e) were immobilized onto the surface of electrode. As expected, the obvious DPV current signal was detected while the signal probe (Cu-ZrMOF@Aptamer@DNA) was connected on the electrode surface (curve f). This indicated that each step of modification of the electrode would not interfere with the detection of *P. aeruginosa*. Next, to investigate the specific binding ability of the aptamer and *P. aeruginosa*, *S. aureus* was chosen as control. In Fig. S2A, *P. aeruginosa* could be specifically bound to the aptamer; whereas, *S. aureus* could not be bound to it (Fig. S2B). In Fig. S2C, the fluorescence intensity of the supernatant of *S. aureus* was approximately six times that of *P. aeruginosa*. This implied that the aptamer can bind to *P. aeruginosa* specifically.

3.4. Optimization of experimental conditions

To obtain the optimal analytical performance of the proposed electrochemical biosensor, the vital parameters of the experiment were optimized, such as the type of working solution, the pH of PBS, the concentration of the antibody against *P. aeruginosa*, the proportion of Cu-ZrMOF and aptamer, the concentration proportion of aptamer and DNA, and the incubation time of the signal probe (Cu-ZrMOF@Aptamer@DNA).

As the common working solutions, PBS and HAc-NaAc were chosen to explore their effects on the catalytic activity of Cu-ZrMOF. In Fig. S3A, the DPV current signal of PBS was about three times that of HAc-NaAc under the same pH condition (pH = 3.0), it might be that PBS contains more free ionic components which improve catalytic activity. The result implied that PBS was more suitable for Cu-ZrMOF. The effect of different pH of PBS ranging from pH 3.0 to pH 6.0 on DPV response was also investigated. As depicted in Fig. S3B, the optimum pH of PBS was 5.0. Given that the concentration of antibody plays an important role in the recognition of *P. aeruginosa*, the DPV current signals were measured at the different concentrations of antibody ranging from 30 μg mL^{-1} to 70 μg mL^{-1}. As a result, the highest current signal was received when the concentration of antibody was 50 μg mL^{-1} (Fig. S3C).

Cu-ZrMOF@Aptamer@DNA, as the signal probe, is a key factor in the process of measurement. The appropriate proportion of Cu-ZrMOF and aptamer is very important for the catalytic effect of the signal probe and the capture effect of *P. aeruginosa*. In Fig. S3D, the current signal was increased with the increasing proportions from 10:1 to 10:2, but it was decreased when the proportions were 10:3 and 10:4. Therefore, 10:2 was chosen as the optimal proportion of Cu-ZrMOF and aptamer. Further, the current signals of different concentration proportions of aptamer and DNA ranging from 1:0.5 to 1:1.5 were investigated. As seen in Fig. S3E, the highest current signal was received when the concentration proportion of aptamer and DNA was 1:1. Finally, the

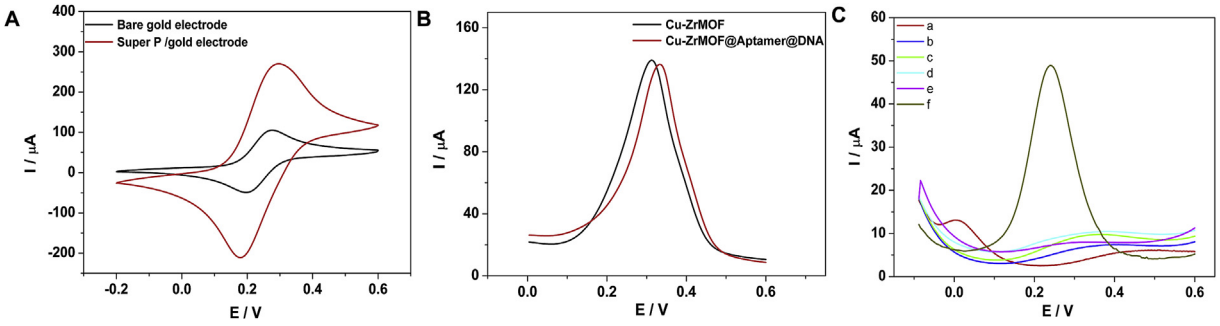

Fig. 3. Investigation of the feasibility of the electrochemical biosensor: (A) CV current signals of gold electrode with and without Super P. (B) DPV current signals of Cu-ZrMOF and Cu-ZrMOF@Aptamer@DNA. (C) DPV current signals of each step of electrode modification: (a) Super P/gold electrode, (b) AuNPs/Super P/gold electrode, (c) antibody/AuNPs/Super P/gold electrode, (d) BSA/antibody/AuNPs/Super P/gold electrode, (e) *P. aeruginosa*/BSA/antibody/AuNPs/Super P/gold electrode, (f) signal probe (Cu-ZrMOF@Aptamer@DNA)/*P. aeruginosa*/BSA/antibody/AuNPs/Super P/gold electrode. (For interpretation of the references to colour in this figure legend, the reader is referred to the Web version of this article.)

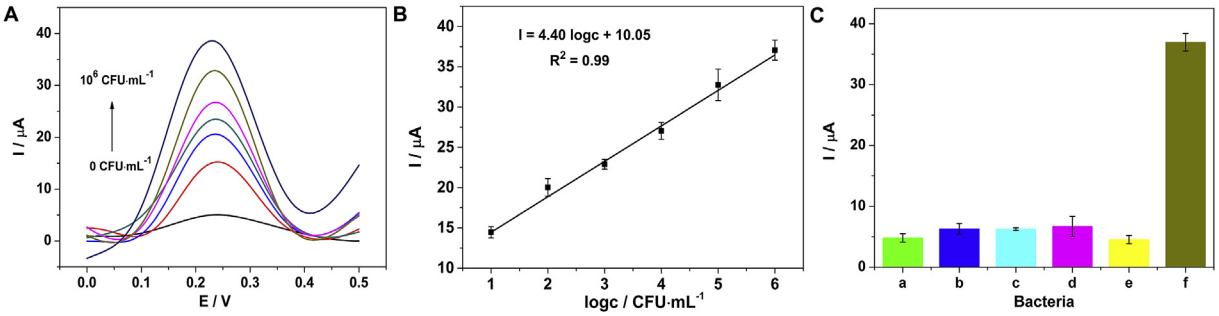

Fig. 4. Analytical performance of the electrochemical biosensor: (A) DPV current signals of different concentrations of *P. aeruginosa*. (B) Linearity of the current signal among different concentrations of *P. aeruginosa*. (C) Current signals of the proposed electrochemical biosensor towards different bacterial strains: (a) blank control, (b) *E. coli*, (c) *A. baumannii*, (d) *S. aureus*, (e) *K. pneumoniae*, (f) *P. aeruginosa*. Error bars = SD (n = 5).

incubation time of Cu-ZrMOF@Aptamer@DNA was also explored. The DPV current signal was gradually increased with the prolongation of the incubation time from 30 min to 50 min, but it exhibited no obvious change when the incubation time was further prolonged to be 60 min (Fig. S3F). Therefore, the optimal incubation time was found to be 50 min.

3.5. Analytical performance of the proposed electrochemical biosensor

3.5.1. Repeatability

As a new method, the repeatability is a very important parameter. The repeatability of proposed electrochemical biosensor was evaluated by relative standard deviation (RSD). As shown in Fig. S4, the current signals were measured repeatedly with different concentrations of *P. aeruginosa* (10^2, 10^4 and 10^6 CFU mL^{-1}), and the RSD were 4.0%, 3.8% and 3.7%, respectively (n = 10).

3.5.2. Linearity range and limit of detection

Under the optimal experimental conditions, different concentrations of *P. aeruginosa* were detected by the electrochemical biosensor. As shown in Fig. 4A, the peak current signal was increased gradually with the increasing concentration of *P. aeruginosa*. The current signal intensity had a good linear relationship with the logarithm of *P. aeruginosa* concentrations ranging from 10 to 10^6 CFU mL^{-1} (Fig. 4B). This indicated that the *P. aeruginosa* could be quantified using the linear regression equation $I\ (\mu A) = 4.40 \log c + 10.05$ with a linear correlation coefficient (R^2) of 0.99. The limit of detection (LOD) was estimated to be 2 CFU mL^{-1} (S/N = 3, n = 10), which was calculated by the following equation: LOD = 3 SD/k (SD represents the standard deviation of the blank, k represents the slope of the linear regression equation) (Feng et al., 2017). As shown in Table S2, compared with the recent literatures regarding the detection of *P. aeruginosa*, the present electrochemical biosensor had good performance with respect to LOD and linearity range. This indicated that the proposed biosensor exhibited good analytical performance for quantifying *P. aeruginosa*.

3.5.3. Specificity

To assess the specificity of the proposed electrochemical biosensor, different bacterial strains at the same concentration (10^6 CFU mL^{-1}) were detected under the same experimental conditions including *E. coli*, *S. aureus*, *A. baumannii* and *K. pneumoniae*. As shown in Fig. 4C, the current signals of those non-target bacterial strains were the same as that of blank control. However, a remarkable current signal was observed only in response to the existence of *P. aeruginosa*. This indicated that the proposed biosensor had a high specificity towards *P. aeruginosa*.

3.5.4. Storage stability

The storage stability was studied by measuring the current signal with the same concentration (10^5 CFU mL^{-1}) of *P. aeruginosa* after the electrochemical biosensor was stored at 4 °C for 7 days and 14 days. In Table S3, compared with the initial current signal of the biosensor, 98.1% and 83.9% of the current signal was retained after storage for 7 days and 14 days, respectively (n = 3). These results indicated that the biosensor had acceptable storage stability within 7 days of storage at 4 °C.

3.6. Analysis of urine samples

To verify the feasibility of the proposed electrochemical biosensor in the clinical setting, it was used to quantify *P. aeruginosa* in urine. The urine samples were spiked with *P. aeruginosa* at concentrations of 10, 10^3 and 10^5 CFU mL^{-1}. Then these urine samples were quantified by the proposed biosensor. The recovery rates were calculated as 96.9%–102.3% with RSD ranging from 3.8% to 4.1% (n = 5), as shown in Table 1. This indicated that the proposed biosensor offered good accuracy for complex matrix samples and had great potential to detect *P. aeruginosa* in clinical application.

4. Conclusion

In present study, a novel enzyme-free electrochemical biosensor was constructed to detect *P. aeruginosa* rapidly and sensitively. The present biosensor was based on the signal amplification strategy utilizing the high catalytic activity of Cu-ZrMOF and the high conductivity of Super P and AuNPs. Due to the combined merits of those materials, the novel biosensor had a wide detection range and a low LOD of 2 CFU mL^{-1} (S/N = 3). Furthermore, quantification of *P. aeruginosa* could be completed within 120 min. Notably, the biosensor platform could also be used to detect other biological targets, including cells, tumour markers and other bacterial strains, of course, the specific recognition element of these targets should be altered consequently. Certainly, the present method still has its limitations. For example, the storage stability of the

Table 1
The recovery test results of the electrochemical biosensor for detecting *P. aeruginosa*.

Sample No.	Spiked *P. aeruginosa* (CFU·mL^{-1})	Detected *P. aeruginosa* (CFU·mL^{-1})	Recovery[a] (%)	RSD (%, n = 5)
1	10	9.7	96.9	3.8
2	1000	1023	102.3	4.1
3	100000	98800	98.8	4.0

[a] Recovery (%) is expressed as the ratio of detected/spiked *P. aeruginosa*.

biosensor needs to be prompted. And the present method is not assembled into a portable point-of-care testing device for clinical use directly. Further studies aim to prompt the storage stability by optimizing additional parameters, and simplify biosensor for assembling into a portable device.

Conflict of interest

None.

Declaration of interests

The authors declare that they have no known competing financial interests or personal relationships that could have appeared to influence the work reported in this paper.

CRediT authorship contribution statement

Xin Zhang: Investigation, Data curation, Formal analysis, Methodology, Visualization, Writing - original draft. **Guoming Xie:** Supervision, Validation, Visualization, Writing - review & editing. **Dan Gou:** Investigation, Data curation, Methodology, Writing - original draft. **Peng Luo:** Conceptualization, Resources, Funding acquisition. **Yuan Yao:** Investigation, Methodology, Data curation. **Hui Chen:** Funding acquisition, Project administration, Resources, Supervision, Validation, Writing - review & editing.

Acknowledgments

This research work was financially supported by the National Natural Science Foundation of China (No. 8167211, No. 81501834).

Appendix A. Supplementary data

Supplementary data to this article can be found online at https://doi.org/10.1016/j.bios.2019.111486.

References

Chen, M., Gan, N., Zhou, Y., Li, T., Xu, Q., Cao, Y., Chen, Y., 2017. Sensor. Actuator. B Chem. 242, 1201–1209.
Chen, W.H., Vazquez-Gonzalez, M., Kozell, A., Cecconello, A., Willner, I., 2018. Small 14 (5), 1703149.
da Silva, L.M.G., Lemos, H.G., Santos, S.F., Antunes, R.A., Venancio, E.C., 2018. Mater. Today. Commun. 16, 14–21.
El-Naggar, M.E., Shaheen, T.I., Fouda, M.M., Hebeish, A.A., 2016. Carbohydr. Polym. 136, 1128–1136.
Feng, C., Bo, B., Mao, X., Shi, H., Zhu, X., Li, G., 2017. Theranostics 7 (1), 31–39.
Gou, D., Xie, G., Li, Y., Zhang, X., Chen, H., 2018. Microchim. Acta. 185 (9), 436–444.
Guo, C., Su, F., Song, Y., Hu, B., Wang, M., He, L., Peng, D., Zhang, Z., 2017. ACS Appl. Mater. Interfaces 9 (47), 41188–41199.
Hassani, S., Akmal, M.R., Salek-Maghsoudi, A., Rahmani, S., Ganjali, M.R., Norouzi, P., Abdollahi, M., 2018. Biosens. Bioelectron. 120, 122–128.
He, C., Lu, K., Liu, D., Lin, W., 2014. J. Am. Chem. Soc. 136 (14), 5181–5184.
Hu, J., Fu, K., Bohn, P.W., 2018. Anal. Chem. 90 (3), 2326–2332.
Huo, X., Liu, P., Zhu, J., Liu, X., Ju, H., 2016. Biosens. Bioelectron. 85, 698–706.
Ito, T., Sekizuka, T., Kishi, N., Yamashita, A., Kuroda, M., 2018. Gut Microb. 10 (1), 77–91.
Jia, F., Xu, L., Yan, W., Wu, W., Yu, Q., Tian, X., Dai, R., Li, X., 2017. Microchim. Acta. 184 (5), 1539–1545.
Kaneti, Y.V., Tang, J., Salunkhe, R.R., Jiang, X., Yu, A., Wu, K.C., Yamauchi, Y., 2017. Adv. Mater. 29 (12), 1604898.
Krithiga, N., Viswanath, K.B., Vasantha, V.S., Jayachitra, A., 2016. Biosens. Bioelectron. 79, 121–129.
Kunze, A., Dilcher, M., Abd El Wahed, A., Hufert, F., Niessner, R., Seidel, M., 2016. Anal. Chem. 88 (1), 898–905.
Li, Y., Xie, G., Qiu, J., Zhou, D., Gou, D., Tao, Y., Li, Y., Chen, H., 2018. Sensor. Actuator. B Chem. 258, 803–812.
Li, Y., Xiong, Y., Fang, L., Jiang, L., Huang, H., Deng, J., Liang, W., Zheng, J., 2017. Theranostics 7 (4), 935–944.
Liu, Y., Hou, W., Xia, L., Cui, C., Wan, S., Jiang, Y., Yang, Y., Wu, Q., Qiu, L., Tan, W., 2018. Chem. Sci. 9 (38), 7505–7509.
Meng, H.M., Liu, H., Kuai, H., Peng, R., Mo, L., Zhang, X.B., 2016. Chem. Soc. Rev. 45 (9), 2583–2602.
Mougous, J.D., Cuff, M.E., Raunser, S., Shen, A., Zhou, M., Gifford, C.A., Goodman, A.L., Joachimiak, G., Ordonez, C.L., Lory, S., Walz, T., Joachimiak, A., Mekalanos, J.J., 2006. Science 312 (5779), 1526–1530.
Shah, N., Naseby, D.C., 2015. Biosens. Bioelectron. 68, 447–453.
Tang, S., Shen, H., Hao, Y., Huang, Z., Tao, Y., Peng, Y., Guo, Y., Xie, G., Feng, W., 2018. Biosens. Bioelectron. 104, 72–78.
Tang, Y., Ali, Z., Zou, J., Jin, G., Zhu, J., Yang, J., Dai, J., 2017. RSC Adv. 7 (82), 51789–51800.
Wang, S., McGuirk, C.M., Ross, M.B., Wang, S., Chen, P., Xing, H., Liu, Y., Mirkin, C.A., 2017a. J. Am. Chem. Soc. 139 (29), 9827–9830.
Wang, X., Yang, C., Zhu, S., Yan, M., Ge, S., Yu, J., 2017b. Biosens. Bioelectron. 87, 108–115.
Yan, Z., Wang, F., Deng, P., Wang, Y., Cai, K., Chen, Y., Wang, Z., Liu, Y., 2018. Biosens. Bioelectron. 109, 132–138.
Yang, J., Shen, H., Zhang, X., Tao, Y., Xiang, H., Xie, G., 2016. Biosens. Bioelectron. 77, 1119–1125.
Yue, H., He, Y., Fan, E., Wang, L., Lu, S., Fu, Z., 2017. Biosens. Bioelectron. 94, 429–432.
Zhang, W., Zong, L., Liu, S., Pei, S., Zhang, Y., Ding, X., Jiang, B., Zhang, Y., 2019. Biosens. Bioelectron. 131, 200–206.
Zhou, D., Xie, G., Cao, X., Chen, X., Zhang, X., Chen, H., 2016. Microchim. Acta. 183 (10), 2753–2760.